

# Assessing DFT-D3 Damping Functions Across Widely Used Density Functionals: Can We Do Better?

Jonathon Witte,<sup>†,‡,§</sup> Narbe Mardirossian,<sup>†</sup> Jeffrey B. Neaton,<sup>‡,§</sup> and Martin Head-Gordon<sup>\*,†,||</sup>

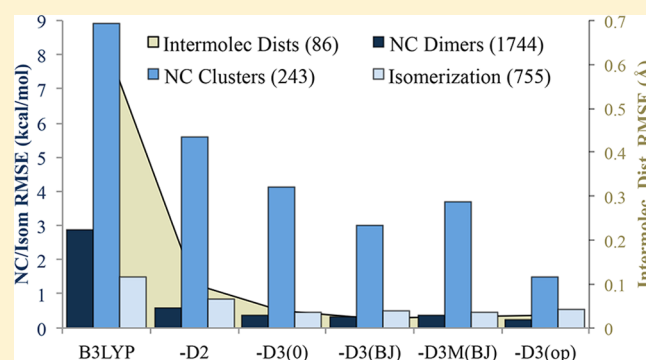
<sup>†</sup>Department of Chemistry and <sup>||</sup>Department of Physics, University of California, Berkeley, California 94720, United States

<sup>‡</sup>Molecular Foundry and <sup>||</sup>Chemical Sciences Division, Lawrence Berkeley National Laboratory, Berkeley, California 94720, United States

<sup>§</sup>Kavli Energy Nanosciences Institute at Berkeley, Berkeley, California 94720, United States

## S Supporting Information

**ABSTRACT:** With the aim of improving the utility of the DFT-D3 empirical dispersion correction, we herein generalize the DFT-D3 damping function by optimizing an additional parameter, an exponent, which controls the rate at which the dispersion tail is activated. This method – DFT-D3(op), shorthand for “optimized power,” where power refers to the newly introduced exponent – is then parametrized for use with ten popular density functional approximations across a small set of noncovalent interactions and isomerization energies; the resulting methods are then evaluated across a large independent test set of 2475 noncovalent binding energies and isomerization energies. We find that the DFT-D3(op) tail represents a substantial improvement over existing damping functions, as it affords significant reductions in errors associated with noncovalent interaction energies and geometries. The revPBE0-D3(op) and MS2-D3(op) methods in particular stand out, and our extensive testing indicates they are competitive with other modern density functionals.



## 1. INTRODUCTION

Kohn–Sham density functional theory (DFT)<sup>1</sup> is the most widely used formalism in electronic structure theory, a consequence of its relative simplicity and the nice balance it strikes between computational expense and accuracy. Nevertheless, DFT has its drawbacks. Although there is a degree of hierarchy within DFT, as exemplified by the proverbial Jacob’s ladder of DFT,<sup>2</sup> there is no prescription for systematically improving results. Moreover, standard approximations within the formalism are inherently semilocal and hence incapable of correctly describing long-range electron correlation, i.e. strong correlations and dispersion forces.<sup>3</sup> This latter deficiency is particularly troubling, since dispersion is integral to the correct description of noncovalent interactions. To address this issue, a “stairway” of dispersion corrections has been constructed over the years.<sup>4</sup>

The simplest such corrections can be traced back to a Hartree–Fock+D approach,<sup>5,6</sup> which, channeling second-order Rayleigh–Schrödinger perturbation theory, adds in a pairwise atomic correction involving empirical isotropic dispersion coefficients with the correct  $r^{-6}$  asymptote. This scheme was later adapted to DFT,<sup>7</sup> which introduced an additional complication: since DFT already describes local electron correlation, the added + D component needs to be damped at small separations in order to avoid double counting. Grimme systematized this approach, first with his introduction of the

DFT-D method<sup>8</sup> and then subsequently DFT-D2<sup>9</sup> and DFT-D3.<sup>10</sup> These methods are widely used for the same reason that DFT is so prolific within the electronic structure community: they are simple, incredibly efficient, and quite accurate for a variety of interesting systems.

In recent years, a number of additional approaches to dispersion have been developed. Von Lilienfeld et al.<sup>11</sup> proposed adding in dispersion-corrected atom-centered potentials (DCACPs) within the effective core-potential approximation; this approach was later adapted to atom-centered basis sets in what is now known as the DCP approach.<sup>12</sup> Several approaches for self-consistently calculating dispersion coefficients have been introduced, most notably the exchange-dipole moment (XDM) model<sup>13–16</sup> and the TS-vdW method.<sup>17</sup> The past decade has even seen the proliferation of methods that attempt to explicitly incorporate nonlocal correlation, such as the vdW-DF<sup>18</sup> and vdW-DF2<sup>19</sup> approaches, which are popular within the solid-state community, and the VV09<sup>20</sup> and VV10<sup>21</sup> methods. For a more thorough description of these various methods, the reader is referred to a recent review by Klimeš and Michaelides.<sup>4</sup>

Within this study, we focus on the most computationally inexpensive brand of dispersion corrections, the aforemen-

Received: February 18, 2017

Published: April 10, 2017



tioned DFT-D2 and DFT-D3 approaches. Specifically, we explore the effect of including an additional degree of freedom within the -D3 damping function, thereby introducing a new, more general damping function. This new damping function is then optimized for several popular density functionals, and the resulting methods are compared to those obtained with existing -D3 damping functions. We find that this new iteration, which we term DFT-D3(op), shorthand for optimized power, substantially improves the description of noncovalent interactions – particularly those involving molecular clusters – and isomerization energies.

## 2. THEORY

Within the DFT-D family of methods, the two-body component of the empirical dispersion energy is given by

$$E^{(2)} = - \sum_{i < j} \sum_{n=6,8,10,\dots} s_n \frac{C_{n,ij}}{r_{ij}^n} f_{\text{damp},n}(r_{ij}) \quad (1)$$

The first sum in eq 1 runs over all unique pairs of atoms  $i$  and  $j$ ;  $C_{n,ij}$  are isotropic  $n$ th-order dispersion coefficients for atom pair  $ij$ ;  $r_{ij}$  is the internuclear distance between atoms  $i$  and  $j$ ;  $s_n$  are global, density functional-dependent scaling parameters; and  $f_{\text{damp},n}(r_{ij})$  are damping functions intended to address small- $r_{ij}$  singularities, as well as double-counting of correlation effects. Early iterations of these dispersion models – namely the original DFT-D,<sup>7,8</sup> as well as DFT-D2<sup>9</sup> – truncated the sum at  $n = 6$ , employed chemically insensitive, pretabulated dispersion coefficients  $C_{6,ij}$  and sums of atomic van der Waals radii  $r_{0,ij}$  and utilized Fermi-type damping functions of the form

$$f_{\text{damp},6}^{\text{D2}}(r_{ij}) = \left[ 1 + \exp \left( -\alpha \left( \frac{r_{ij}}{r_{0,ij}} - 1 \right) \right) \right]^{-1} \quad (2)$$

with  $\alpha$  generally fixed to 20.

In 2010, Grimme et al.<sup>10</sup> introduced the now widely used DFT-D3 scheme. Although many aspects of -D3 are similar to -D2, there are some key fundamental differences: a counting function is introduced to allow the  $C_{6,ij}$  coefficients to be weakly environmentally dependent; the sum in eq 1 is extended to include the  $n = 8$  term, and a CHG-style<sup>22</sup> damping function – given in eq 3 – is used. For the damping function, Grimme et al.<sup>10</sup> chose to fix  $s_{r,8} = 1$ ,  $\alpha_6 = 14$ , and  $\alpha_8 = 16$ , thereby optimizing only one nonlinear parameter –  $s_{r,6}$  – for each density functional. Moreover, for almost all density functionals,  $s_6$  is fixed to unity, leaving only one linear parameter,  $s_8$ . This version of DFT-D3 is now known as zero-damping or DFT-D3(0).

$$f_{\text{damp},n}^{\text{D3(0)}}(r_{ij}) = \left[ 1 + 6 \left( \frac{r_{ij}}{s_{r,n} r_{0,ij}} \right)^{-\alpha_n} \right]^{-1} \quad (3)$$

One year later, Grimme et al.<sup>23</sup> combined the basic principles of DFT-D3 with the finite-damping scheme Johnson and Becke<sup>15</sup> had utilized in their XDM approach to dispersion; this is now the generally preferred style of -D3, termed DFT-D3(BJ). The damping function is of the form

$$f_{\text{damp},n}^{\text{D3(BJ)}}(r_{ij}) = \frac{r_{ij}^n}{r_{ij}^n + (\alpha_1 r_{0,ij} + \alpha_2)^n} \quad (4)$$

where  $\alpha_1$  and  $\alpha_2$  are adjustable nonlinear parameters. At short internuclear distances  $r_{ij}$ , the dispersion energy  $E^{(2)}$  in the zero-damping approach vanishes, since  $f_{\text{damp},n}(r_{ij})$  decays more quickly than  $C_{n,ij} r_{ij}^{-n}$ . In the BJ-damping scheme, however, these two terms decay at the same rate, and hence  $E^{(2)}$  asymptotes to a finite value. This is the key difference between the -D3(0) and -D3(BJ) approaches. Although van der Waals radii  $r_{0,ij}$  in -D3(BJ) are given by  $\sqrt{\frac{C_{8,ij}}{C_{6,ij}}}$  instead of their -D3(0) values, the tabulated coefficients  $C_{n,ij}$  are the same, and – as with -D3(0) –  $s_6$  is generally fixed to unity in -D3(BJ), leaving  $s_8$  as the sole linear parameter.

This new version of -D3 with BJ-damping has become the preferred version of -D3 due to the fact that it consistently outperforms -D3(0).<sup>23</sup> Recently, Schröder et al.<sup>24</sup> have attempted to simplify the model with their C-Six-Only (CSO) approach, wherein they introduce a sigmoidal interpolation function to approximate the eighth-order term. In so doing, they eliminate one linear parameter and one nonlinear parameter without significantly impacting performance across GMTKN30 or S66.<sup>24</sup> The damping function for this approach, -D3(CSO), is given by

$$f_{\text{damp},6}^{\text{D3(CSO)}}(r_{ij}) = \frac{r_{ij}^6}{r_{ij}^6 + (\alpha_3 r_{0,ij} + \alpha_4)^6} \left[ 1 + \frac{\alpha_1}{s_6 [1 + \exp(r_{ij} - \alpha_2 r_{0,ij})]} \right] \quad (5)$$

Note the similarities between eqs 4 and 5:  $\alpha_3$  and  $\alpha_4$  in the CSO scheme correspond to  $\alpha_1$  and  $\alpha_2$  in BJ-damping, respectively, and the bracketed term in eq 5 is the interpolation function. For the density functionals they examined, Schröder et al.<sup>24</sup> found  $\alpha_3 \approx 0$ ,  $\alpha_4 \approx 6.25$ , and  $\alpha_2 \approx 2.5$ , leaving  $\alpha_1$  as the sole functional-dependent parameter in -D3(CSO).

In addition to the dispersion corrections mentioned thus far, we consider in this work the modified version of -D3(BJ) recently proposed by Smith et al.<sup>25</sup> The damping function in this approach, -D3M(BJ), is identical to that in eq 4; the method constitutes a refitting of the BJ-damping parameters to a much broader set of data. Grimme et al.<sup>23</sup> originally fit  $s_8$ ,  $\alpha_1$ , and  $\alpha_2$  on 130 data points; Smith et al.<sup>25</sup> utilize a training set of 1526 energies, with an emphasis on nonequilibrium – particularly compressed – geometries.

It is illustrative to rewrite the damping function for -D3(0) from eq 3. By doing so, we obtain

$$f_{\text{damp},n}^{\text{D3(0)}}(r_{ij}) = \frac{r_{ij}^{\alpha_n}}{r_{ij}^{\alpha_n} + (\sqrt[n]{6} s_{r,n} r_{0,ij})^{\alpha_n}} \quad (6)$$

The similarities between the functional forms of -D3(0) and -D3(BJ) are striking (cf. eqs 4 and 6). There is a direct correspondence between  $\alpha_1$  in BJ-damping and  $s_{r,n}$ . Whereas in -D3(BJ)  $\alpha_1$  is the same for the sixth- and eighth-order terms, in -D3(0) this is no longer the case, as  $s_{r,6} \neq s_{r,8}$ . The original zero-damping scheme thus resembles a slightly constrained version of BJ-damping, wherein  $\alpha_2$  (the constant added to the van der Waals radii) is zero, and the sixth-order power is 14 instead of 6.

In this work, we generalize the BJ-damping function, adding a parameter to control how quickly the damping occurs, i.e. the power. The damping function we employ is given by

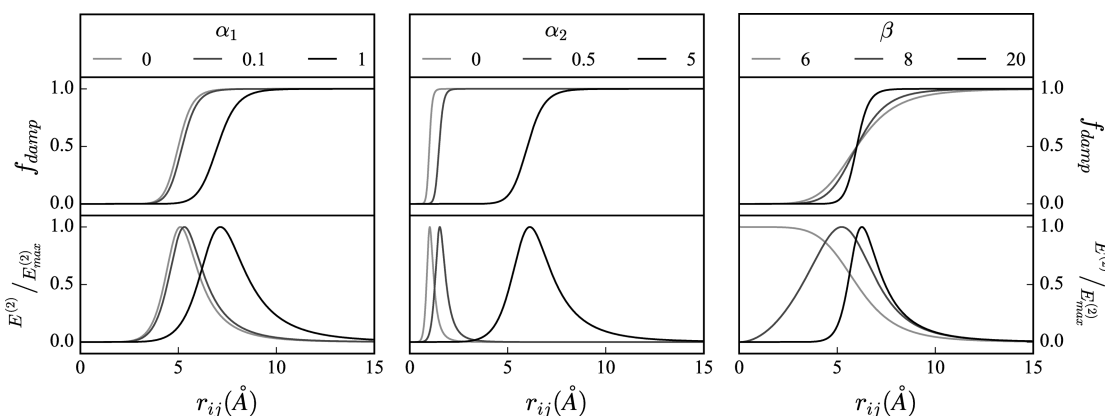


**Figure 1.** Visualization of the effects of varying parameters  $\alpha_1$ ,  $\alpha_2$ , and  $\beta$  from eq 7. The leftmost plots are generated by varying  $\alpha_1$  with fixed  $\alpha_2$  and  $\beta$ ; the center plots are generated by varying  $\alpha_2$  with fixed  $\alpha_1$  and  $\beta$ ; and the rightmost plots are generated by varying  $\beta$  with fixed  $\alpha_1$  and  $\alpha_2$ . When not being varied, the parameters are fixed to  $\alpha_1 = 0.5$ ,  $\alpha_2 = 5$ , and  $\beta = 14$ , with  $r_{0,ij} = 2$  Å. The top plot in each section shows the damping function for the sixth-order term,  $f_{\text{damp},6}^{\text{D3(op)}}(r_{ij})$  from eq 7. The bottom plot in each section shows the sixth-order contribution to the two-body dispersion energy,  $E^{(2)}$ , which has been normalized to span the range  $[0,1]$ .

$$f_{\text{damp},n}^{\text{D3(op)}}(r_{ij}) = \frac{r_{ij}^{\beta_n}}{r_{ij}^{\beta_n} + (\alpha_1 r_{0,ij} + \alpha_2)^{\beta_n}} \quad (7)$$

This new scheme – optimized-power-damping, or -D3(op) – is mathematically similar to both BJ-damping and zero-damping. As is the case with both BJ- and zero-damping, we constrain  $\beta_8 = \beta_6 + 2$ . We utilize the same isotropic dispersion coefficients as both -D3(0) and -D3(BJ), the same van der Waals radii as -D3(BJ) – i.e.  $r_{0,ij} = \frac{C_{8,ij}}{C_{6,ij}}$  – and optimize three nonlinear parameters ( $\alpha_1$ ,  $\alpha_2$ ,  $\beta = \beta_6$ ) and one linear parameter ( $s_8$ ). The effects of varying the nonlinear parameters in this model are visualized in Figure 1. The holdovers from BJ-damping –  $\alpha_1$  and  $\alpha_2$  – primarily control the distance  $r_{ij}$  at which the damping function switches off the dispersion correction:  $\alpha_1$  and  $\alpha_2$  are just multiplicative and additive terms, respectively, for the sum of van der Waals radii  $r_{0,ij}$ . The newly introduced  $\beta$ , on the other hand, controls the rate at which the dispersion correction is switched off; in the limit  $\beta \rightarrow \infty$ ,  $f_{\text{damp}}(r_{ij}) \rightarrow \theta(r_{ij})$ , i.e. the damping function just becomes a step function. Most small changes in  $\beta$  correspond to subtle changes in the dispersion energy,  $E^{(2)}$ ; the exception is the transition from  $\beta = 6$  to  $\beta = 6 + \epsilon$ , which is a fundamentally different change than that from, say,  $\beta = 10$  to  $\beta = 10 + \epsilon$ . For all  $\beta > 6$ , the contribution of atom pair  $ij$  to the dispersion energy at  $r_{ij} = 0$  is zero; for  $\beta = 6$ , this contribution is nonzero. In practice, however, this difference is not so significant; due to Pauli repulsion, the limit  $r_{ij} = 0$  is not particularly meaningful.

An overview of the six forms of dispersion corrections considered in this study – -D2, -D3(0), -D3(BJ), -D3M(BJ), -D3(CSO), and -D3(op) – can be found in Table 1. Note we have not considered the modified version of zero-damping, -D3M(0), as it was found to be inferior to -D3M(BJ) by the original authors.<sup>25</sup>

### 3. COMPUTATIONAL DETAILS

We have optimized the DFT-D3(op) damping function given in eq 7 for several density functional approximations and compared its performance to that of existing damping functions. Specifically, we have considered the ten density functionals outlined in Table 2.

**Table 1. Summary of Empirical Dispersion Corrections Considered in This Study**

type	fit parameters		$C_8?$	ref
	linear	nonlinear		
-D2	$s_6$	none	no	9
-D3(0)	$s_8$	$s_{r,6}$	yes	10
-D3(BJ)	$s_8$	$\alpha_1, \alpha_2$	yes	23
-D3M(BJ)	$s_8$	$\alpha_1, \alpha_2$	yes	25
-D3(CSO)	none	$\alpha_1$	no	24
-D3(op)	$s_6$ or $s_8$	$\alpha_1, \alpha_2, \beta$	maybe	this work

**Table 2. Summary of Density Functionals<sup>a</sup>**

functional	class	empirical dispersion	ref
BLYP	GGA	D2, D3(0), D3(BJ), D3M(BJ), D3(CSO)	27, 28
B3LYP	hybrid GGA	D2, D3(0), D3(BJ), D3M(BJ), D3(CSO)	27–30
B97	GGA	D2, D3(0), D3(BJ), D3M(BJ)	9
B97h	hybrid GGA	D2	26
revPBE	GGA	D3(0), D3(BJ)	31, 32
revPBE0	hybrid GGA	D3(0), D3(BJ)	31–33
TPSS	meta-GGA	D2, D3(0), D3(BJ), D3(CSO)	34
TPSSh	hybrid meta-GGA	D3(0), D3(BJ)	35
MS2	meta-GGA	D3(0)	36
MS2h	hybrid meta-GGA	D3(0)	36

<sup>a</sup>The names in the first column are standard, with two exceptions: B97 corresponds to Grimme’s pure functional B97-D,<sup>9</sup> which has had the dispersion tail stripped away, and B97h corresponds to the original hybrid functional B97, as parameterized by Becke.<sup>26</sup> The third column details the existing parameterized DFT-D-style dispersion corrections we consider in this study, and the fourth column lists the references for the method.

These ten representative density functionals were carefully chosen. There are five natural pairs of pure/hybrid functionals: BLYP/B3LYP, B97/B97h, revPBE/revPBE0, TPSS/TPSSh, and MS2/MS2h. The first three of these pairs are generalized gradient approximations (GGAs), and the last two are meta-GGAs. Moreover, each of these ten density functionals exhibits positive mean signed errors across every data set of noncovalent

Table 3. Summary of Data Sets That Comprise the Training and Test Sets<sup>a</sup>

set	datatype	no.	constituent data sets	ref
train	NCED	127	S66, HB49, AlkBind12	44–49
	NCEC	18	H2O6Bind8, H2O20Bind4, HW6Cl	50–55
	IE	122	Butanediol65, Melatonin52, H2O16Rel5	56–58
	BL	20	interpolated equilibrium binding lengths from BzDC215 and NBC10	59–63
test	NCED	1617	A24, DS14, HB15, HSG, NBC10, S22, X40, A21x12, BzDC215, HW30, NC15, S66x8, 3B-69-DIM, CO2Nitrogen16, Ionic43	45, 59–75
	NCEC	225	HW6F, FmH2O10, Shields38, SW49Bind345, SW49Bind6, WATER27, 3B-69-TRIM, CE20, H2O20Bind10	50–53, 73, 76–79
	NCD	91	TA13, XB18, Bauza30, CT20, XB51	80–84
	IE	633	AlkIsomer11, ACONF, CYCONF, Pentane14, SW49Rel345, SW49Rel6, H2O20Rel10, H2O20Rel4, YMPJ519	51–53, 55, 77, 85–89
	ID	155	EIE22, Styrene45, DIE60, ISOMERIZATION20, C20C24	78, 90, 92
	TCE	947	AlkAtom19, BDE99nonMR, G21EA, G21IP, TAE140nonMR, AlkIsod14, BH76RC, EA13, HAT707nonMR, IP13, NBPRC, SN13, BSR36, HNBBrBDE18, WCPT6	53, 85, 91, 93–101
	TCD	258	BDE99MR, HAT707MR, TAE140MR, PlatonicHD6, PlatonicID6, PlatonicIG6, PlatonicTAE6	91, 102
	BH	206	BHPERI26, CRBH20, DBH24, CR20, HTBH38, NHTBH38, PX13, WCPT27	53, 78, 79, 94, 95, 101, 103–107

<sup>a</sup>For more details, see ref 43.

interactions we considered; that is to say, they consistently underbind every type of system at which we have looked and hence can all profit greatly from the addition of a dispersion correction. One popular functional we excluded from this study is PBE. Since PBE is known to overbind water clusters,<sup>37</sup> we believe it is not a good candidate for a blanket dispersion correction. That being said, although PBE (and its complement, PBE0) is not found within the main study, parametrizations for both may be found in the [Supporting Information](#).

All density functional calculations were performed without counterpoise correction in the def2-QZVPPD basis,<sup>38,39</sup> near the basis set limit for standard noncovalent interactions.<sup>40</sup> A fine Lebedev integration grid consisting of 99 radial shells – each with 590 angular points – was utilized in the computation of all semilocal components of exchange and correlation; nonlocal correlation in the VV10-containing functionals was calculated with the coarser SG-1 grid.<sup>41</sup> All calculations were performed within a development version of Q-Chem 4.4.<sup>42</sup>

For each density functional, we performed an exhaustive determination of the optimal parameters for the DFT-D3(op) method. Specifically, we scanned  $\alpha_1$  from 0 to 1 in steps of 0.025,  $\alpha_2$  from 0 to 10 in increments of 0.25, and  $\beta$  from 6 to 18 in increments of 2; this resulted in 11767 possible forms of the -D3(op) tail for each density functional.

To identify the best of these many candidate fits, we utilized the comprehensive database assembled by Mardirossian and Head-Gordon.<sup>43</sup> This database contains 4399 data points which are spread out among 82 smaller data sets. These smaller constituent data sets are classified according to eight distinct datatypes: NCED (easy noncovalent interactions of dimers), NCEC (easy noncovalent interactions of clusters), NCD (difficult noncovalent interactions of dimers), IE (easy isomerization energies), ID (difficult isomerization energies), TCE (easy thermochemistry), TCD (difficult thermochemistry), and BH (barrier heights). “Difficult” interactions involve either strong correlation or self-interaction error, whereas “easy” interactions are not heavily characterized by either. In order to facilitate the testing of -D3(op) candidates, the data sets were divided into two categories. A training set was used to identify the best set of parameters, and a test set was used to assess the performance of the resulting method relative to existing dispersion corrections. A summary of the data sets can be found in [Table 3](#).

Once all 11767 possible fits were generated for a given functional, we set  $s_6$  to unity and performed a least-squares fit of  $s_8$  to a small subset of NCEDTrain and IETrain, namely S66 and Butanediol65. The resulting methods were then sorted according to a simple product of root-mean-square errors (RMSEs) across 11 training data sets – S66, HB49, AlkBind12, H2O6Bind8, H2O20Bind4, HW6Cl, Butanediol65, Melatonin52, H2O16Rel5 and two geometric data sets: interpolated equilibrium binding lengths of BzDC215 and NBC10. To prevent the appearance of unphysical parameters (negative values of  $s_8$ ), when  $s_8$  optimized to a value less than 0.1, we set  $s_8 = 0$  and performed a least-squares fit of  $s_6$  instead. The only functional within this study for which this occurred is B97h.

#### 4. RESULTS AND DISCUSSION

In the course of this study, we have introduced a new damping function for use in the DFT-D3 empirical dispersion correction – DFT-D3(op) – which encompasses the space spanned by DFT-D3(BJ) and an unconstrained form of DFT-D3(0). We have optimized this new damping function for ten distinct density functionals across a small yet diverse training set. The resulting optimized fit parameters are listed in [Table 4](#); parametrizations for additional functionals may be found in the [Supporting Information](#).

This new variant of DFT-D3 was then evaluated in tandem with existing versions across a large independent test set. The results are given in [Figure 2](#), within which we show for each

Table 4. Optimized Values of -D3(op) Fit Parameters for Each Density Functional

functional	$s_6$	$s_8$	$\alpha_1$	$\alpha_2$	$\beta$
BLYP	1.00000	1.31867	0.425	3.50	8
B3LYP	1.00000	0.78311	0.300	4.25	10
B97	1.00000	1.46861	0.600	2.50	6
B97h	0.97388	0.00000	0.150	4.25	12
revPBE	1.00000	1.44765	0.600	2.50	6
revPBE0	1.00000	1.25684	0.725	2.25	6
TPSS	1.00000	0.51581	0.575	3.00	14
TPSSH	1.00000	0.43185	0.575	3.00	14
MS2	1.00000	0.90743	0.700	4.00	8
MS2h	1.00000	1.69464	0.650	4.75	6



Functional	Non-Covalent: Dimers			Non-Covalent: Clusters			Isomerization			Equilibrium		Overall Product
	NCED*	HSG	S22	NCEC*	Shields	3B-69	IE*	Pent14	YMPJ	BL (Å)	BE	
<b>BLYP</b>	3.46	3.39	6.00	14.20	7.82	8.39	1.58	0.55	1.51	0.225	3.80	
-D2	0.54	0.48	0.25	2.13	3.23	0.73	1.17	0.83	1.18	0.095	0.58	12.85
-D3(0)	0.36	0.39	0.28	<b>1.67</b>	2.52	0.52	0.83	<b>0.20</b>	0.80	0.028	0.42	1.41
-D3(BJ)	0.33	0.40	0.32	2.07	1.59	0.71	0.71	0.48	0.70	<b>0.027</b>	<b>0.23</b>	1.32
-D3M(BJ)	0.33	<b>0.29</b>	0.34	2.57	3.81	0.69	0.72	0.45	0.71	0.038	0.31	2.33
-D3(CSO)	0.40	0.48	0.38	3.21	<b>0.61</b>	0.80	<b>0.68</b>	0.49	0.65	0.061	0.29	5.29
-D3(op)	<b>0.31</b>	0.40	<b>0.20</b>	1.77	2.24	0.75	0.73	0.41	0.74	0.029	<b>0.21</b>	<b>1.14</b>
<b>B3LYP</b>	2.82	2.68	4.89	8.67	4.54	6.61	1.34	0.47	1.28	0.215	3.12	
-D2	0.58	0.45	0.61	5.19	5.14	0.80	0.89	0.54	0.88	0.100	0.81	26.63
-D3(0)	0.35	0.27	0.42	3.69	4.00	0.79	0.50	0.13	0.45	0.027	0.44	1.71
-D3(BJ)	0.30	0.21	0.43	2.67	3.21	0.74	0.51	0.20	0.49	<b>0.022</b>	0.38	0.89
-D3M(BJ)	0.34	0.19	0.52	3.32	3.79	0.80	0.50	0.19	0.49	0.023	0.44	1.32
-D3(CSO)	0.30	0.25	0.30	1.51	2.15	0.63	<b>0.48</b>	0.20	0.44	0.047	0.28	1.01
-D3(op)	<b>0.26</b>	0.30	<b>0.25</b>	<b>1.28</b>	1.88	0.56	0.55	0.20	0.54	0.027	<b>0.24</b>	<b>0.49</b>
<b>B97</b>	3.66	3.70	6.49	21.42	15.11	9.30	1.87	0.64	1.77	0.239	3.86	
-D2	0.57	0.72	0.62	5.63	3.66	1.42	1.28	0.66	1.33	0.068	0.53	27.50
-D3(0)	<b>0.39</b>	0.50	0.54	4.12	2.22	1.17	0.76	<b>0.08</b>	0.77	0.034	0.35	4.16
-D3(BJ)	0.46	0.55	0.49	4.75	2.75	1.11	0.82	0.28	0.82	0.047	0.38	8.40
-D3M(BJ)	0.40	0.40	0.38	2.75	0.94	1.17	<b>0.61</b>	0.19	0.60	0.032	0.30	2.14
-D3(op)	0.41	0.39	0.38	<b>1.83</b>	0.42	1.08	0.72	0.30	0.70	<b>0.026</b>	<b>0.29</b>	<b>1.38</b>
<b>B97h</b>	2.41	2.26	4.39	10.42	6.50	5.77	1.27	0.41	1.19	0.218	2.56	
-D2	0.49	0.39	0.71	<b>1.14</b>	0.44	0.93	0.72	0.42	0.73	0.045	0.40	1.80
-D3(op)	<b>0.29</b>	0.33	<b>0.44</b>	1.29	0.30	0.55	<b>0.56</b>	0.10	0.59	<b>0.034</b>	<b>0.26</b>	<b>0.71</b>
<b>revPBE</b>	3.61	3.68	6.45	21.85	14.82	9.25	1.76	0.60	1.66	0.238	3.88	
-D3(0)	<b>0.41</b>	0.56	0.61	5.50	2.71	1.12	0.81	<b>0.08</b>	0.84	0.037	0.42	6.67
-D3(BJ)	0.48	0.60	0.62	6.56	3.51	1.25	0.81	0.39	0.81	0.056	0.43	14.08
-D3(op)	0.42	0.39	0.40	<b>2.44</b>	0.42	1.06	<b>0.75</b>	0.41	0.74	<b>0.031</b>	<b>0.30</b>	<b>2.36</b>
<b>revPBE0</b>	3.08	3.14	5.45	16.52	12.07	7.78	1.51	0.58	1.41	0.229	3.38	
-D3(0)	0.32	0.34	0.36	2.14	1.56	0.53	0.59	0.26	0.62	0.032	0.40	1.32
-D3(BJ)	<b>0.32</b>	0.37	<b>0.32</b>	3.44	2.53	0.77	<b>0.56</b>	0.09	0.56	0.037	<b>0.23</b>	2.26
-D3(op)	0.33	0.26	0.39	<b>0.83</b>	0.33	0.80	0.56	0.09	0.55	<b>0.024</b>	0.29	<b>0.37</b>
<b>TPSS</b>	2.53	2.49	4.61	8.81	3.64	6.48	1.22	<b>0.47</b>	1.08	0.217	2.90	
-D2	0.63	0.48	0.64	4.74	5.67	0.89	1.07	0.89	1.03	0.118	0.77	37.47
-D3(0)	0.34	0.25	0.44	2.75	3.90	0.74	<b>0.67</b>	0.38	<b>0.53</b>	0.059	0.35	3.73
-D3(BJ)	0.36	0.26	0.47	1.90	2.85	0.96	0.70	0.55	0.57	0.074	0.34	3.51
-D3(CSO)	0.38	0.25	0.43	1.85	2.69	0.90	0.69	0.56	0.59	0.075	0.33	3.62
-D3(op)	<b>0.32</b>	0.31	0.36	<b>1.76</b>	2.54	0.87	0.78	0.45	0.67	<b>0.053</b>	<b>0.28</b>	<b>2.28</b>
<b>TPSSH</b>	2.46	2.42	4.43	8.33	3.97	6.24	1.19	0.40	1.06	0.214	2.82	
-D3(0)	0.34	0.20	0.49	2.59	3.35	0.74	<b>0.56</b>	0.24	0.46	0.056	0.36	2.77
-D3(BJ)	0.35	0.23	0.44	1.49	2.13	0.86	0.63	0.42	0.53	0.072	0.33	2.37
-D3(op)	<b>0.30</b>	0.27	<b>0.35</b>	<b>1.41</b>	2.02	0.80	0.69	0.31	0.59	<b>0.048</b>	<b>0.28</b>	<b>1.41</b>
<b>MS2</b>	1.24	1.28	2.36	4.83	2.77	3.48	0.68	0.29	0.67	0.126	1.70	
-D3(0)	0.38	0.38	0.41	1.38	1.24	0.62	0.49	0.09	0.41	<b>0.034</b>	0.43	0.86
-D3(op)	<b>0.29</b>	0.19	0.43	<b>0.91</b>	0.29	0.50	<b>0.35</b>	0.11	0.33	0.039	<b>0.23</b>	<b>0.36</b>
<b>MS2h</b>	1.27	1.31	2.36	4.49	2.84	3.50	0.68	0.34	0.67	0.130	1.72	
-D3(0)	0.34	0.33	0.34	1.68	1.14	0.59	0.43	0.12	0.34	0.033	0.39	0.80
-D3(op)	<b>0.26</b>	0.13	0.32	<b>0.56</b>	0.21	0.43	<b>0.27</b>	0.14	0.24	<b>0.027</b>	<b>0.20</b>	<b>0.11</b>

**Figure 2.** Root-mean-square errors across various data sets for all combinations of functionals and dispersion corrections examined. Abbreviations of the data set names are used; the full names are, in order, NCEDTest, HSG, S22, NCECTest, Shields38, 3B-69-TRIM, IETest, Pentane14, YMPJ519, S66x8 BL, and S66x8 BE. The Product column corresponds to a simple product across the aggregate data set RMSEs (times 100). All RMSEs are in units of kcal/mol, with the exception of the equilibrium binding lengths (BL), which are in units of angstroms. Each column within every functional block is color-coded for ease of reading, with darker cells corresponding to lower RMSEs; note, however, that the color-gradient is not uniform but rather skewed to emphasize significant differences among the top fits for each functional. Additionally, the lowest RMSE achieved by any functional-dispersion combination on each aggregate data set is indicated in bold.

method the root-mean-square errors (RMSEs) across the three energetic categories for which empirical dispersion methods are best suited – namely NCEDTest, NCECTest, and IETest – as well as one geometric category, S66x8 interpolated equilibrium binding lengths (and corresponding interpolated equilibrium binding energies). For each of NCEDTest, NCECTest, and IETest, both the aggregate results as well as results for two representative constituent data sets are provided.

From Figure 2, it is evident that the newly proposed -D3(op) dispersion correction represents an improvement over existing corrections for a diverse set of density functionals and systems. Even in cases where the power optimizes to  $\beta = 6$ , which corresponds to the DFT-D3(BJ) scheme, we see large improvements in some categories. This is the case, for instance, for revPBE. Relative to revPBE-D3(BJ), revPBE-D3(op) exhibits significantly lower RMSEs across all metrics related

to noncovalent interactions; the reductions in errors on molecular clusters (NCEC, 63%) and geometries (BL, 45%) are particularly striking. This sort of improvement highlights the benefits a simple reoptimization incorporating the plethora of new high quality data that have been published in the past six years can bring; after all, revPBE-D3(op) is effectively just a reparametrization of revPBE-D3(BJ). Note that for this particular functional, there is no DFT-D3M(BJ) version with which to compare our reparametrization; Smith et al.<sup>25</sup> chose to parametrize PBE instead of revPBE.

Another manifestation of the importance of having a well-balanced training set is the performance of DFT-D3(CSO). In a recent study, it was found that DFT-D3(CSO) reproduces bond lengths and rotational constants quite well.<sup>108</sup> Here, we find that this satisfactory intramolecular performance does not transfer to intermolecular metrics, despite the fact that DFT-

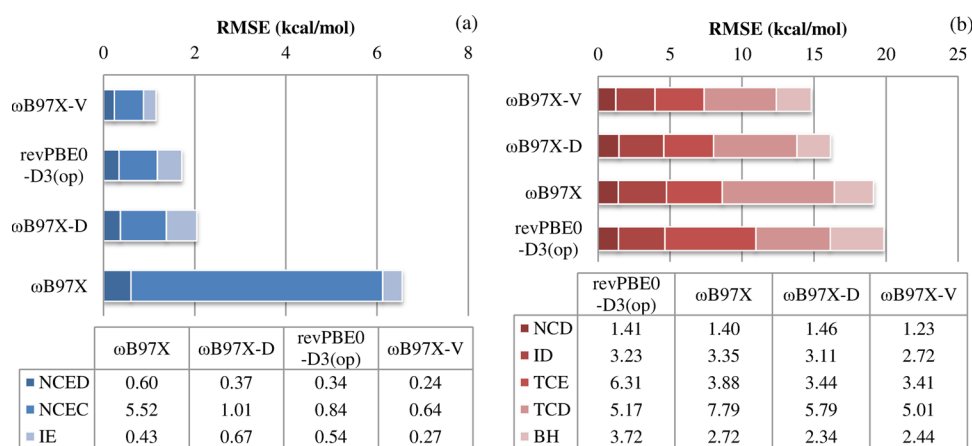


**Figure 3.** Root-mean-square errors (RMSEs) across various datatypes (see Table 3) for the top-performing D3-corrected hybrid GGA functional examined in this work, as well as three other state-of-the-art hybrid GGA functionals. The left plot – (a) – contains data sets pertaining to standard noncovalent interactions and isomerization energies, whereas the right plot – (b) – encompasses other data, such as thermochemistry, which is beyond the realm of a D3 correction. Within each plot, the methods are ordered from best performance across the constituent data sets at the top, to worst performance at the bottom. Tables of RMSEs are provided below the bar graphs to facilitate quantitative comparison.

D3(CSO) is decent at reproducing accurate energies (particularly isomerization energies, at which it seems to excel). Regardless of density functional, -D3(CSO) exhibits significantly larger errors in equilibrium binding lengths than any of the other iterations of -D3; for B3LYP-D3(CSO), for instance, the RMSE across BL is nearly double the next-highest B3LYP-D3 BL RMSE. This is likely a consequence of the fact that DFT-D3(CSO) was trained exclusively on equilibrium systems, specifically S66. This is in stark contrast to other DFT-D3 variants, which were trained on geometries either implicitly through the inclusion of nonequilibrium systems – as was the case for -D3(0), -D3(BJ), and -D3M(BJ) – or by explicitly including geometries in the training metric, as is the case here for -D3(op).

Similarly, deviations among performances across single data sets highlight the need for diverse aggregate data sets. From the exemplary performance of BLYP-D3(CSO) on the Shields38 set, one might infer that this method should be particularly well-suited to water clusters. This is not the case, however; BLYP-D3(CSO) has the highest RMSE of all BLYP-D3 variants across the H2O20Bind10 set of large water clusters by nearly a factor of 2. Oftentimes, outstanding performance of a particular method on a particular set of systems will transfer to similar systems, but that sort of transferability is not guaranteed. The larger and more diverse the independent test set, the more likely the results will be transferable.

This point is further driven home by the relative performances of the DFT-D3(BJ) and -D3M(BJ) methods. For instance, compare B3LYP-D3(BJ) and B3LYP-D3M(BJ) in Figure 2. The -D3M(BJ) method is simply a reparametrization of -D3(BJ) across a significantly larger training set. In the case of B3LYP-D3M(BJ), however, this reparametrization has resulted in significant loss of performance as measured by RMSEs across equilibrium noncovalent interactions. This is likely a consequence of the large emphasis placed on compressed geometries in the parametrization of -D3M(BJ) by both the composition of the data sets and the unique error metric employed.

A consistent feature of functionals employing the DFT-D3(op) tail is enhanced performance on molecular clusters and geometries, as illustrated by low RMSEs across the NCECTest

and S66x8 BL sets. For instance, B97-D3(op) performs similarly to B97-D3(BJ) and B97-D3(0) across NCEDTest and IETest but with dramatic reduction in error across NCECTest and interpolated S66x8 binding lengths. Even in cases where performance on molecular dimers is significantly improved, e.g. B3LYP-D3(op) and MS2h-D3(op), we still see solid performances on clusters and geometries. Whereas with other dispersion tails, performance on molecular clusters is very dependent on the choice of base functional; the -D3(op) approach consistently captures cluster binding energies quite well. For instance, from Figure 2, it is clear that BLYP-D3(0) is the best BLYP-based approach examined on NCECTest, even beating out BLYP-D3(op) by 0.10 kcal/mol; on the other hand, B97-D3(0) has a NCECTest RMSE more than double that of B97-D3(op). This high degree of consistency in the new correction, -D3(op), is likely attributable to the incorporation of molecular clusters in the training set. It is worth noting that a three-body correction of the form suggested by Grimme et al.<sup>10</sup> was also considered in this study; its inclusion, however, did not impact results in any meaningful way. It is quite possible that for larger systems, a three-body term would become relevant.

The one category for which we consistently see the least improvement with the new DFT-D3(op) correction is IETest, i.e. isomerization energies. For certain functionals – most notably MS2 and MS2h – the -D3(op) tail actually improves performance on IETest dramatically. For others, such as TPSS and B3LYP, the new approach is slightly worse than the existing tails – though still significantly better than the base functionals – for isomerization energies. There is inevitably some degree of trade-off between performances across these various properties; of the 11767 combinations of parameters we examined for any given functional, there were certain fits which excelled at one particular category. Although in theory it would be possible to recommend specialized fits for each functional which are best suited for a particular property – B3LYP-D3(op,NCED), B3LYP-D3(op,NCEC), B3LYP-D3(op,IE), etc. – that sort of approach has limited utility. It is far simpler to recommend a parametrization that provides a balanced description of all relevant properties. Comparing B3LYP-D3(op) and B3LYP-D3(BJ), for instance, we see the former has 8% higher RMSE across IETest; however, this slight

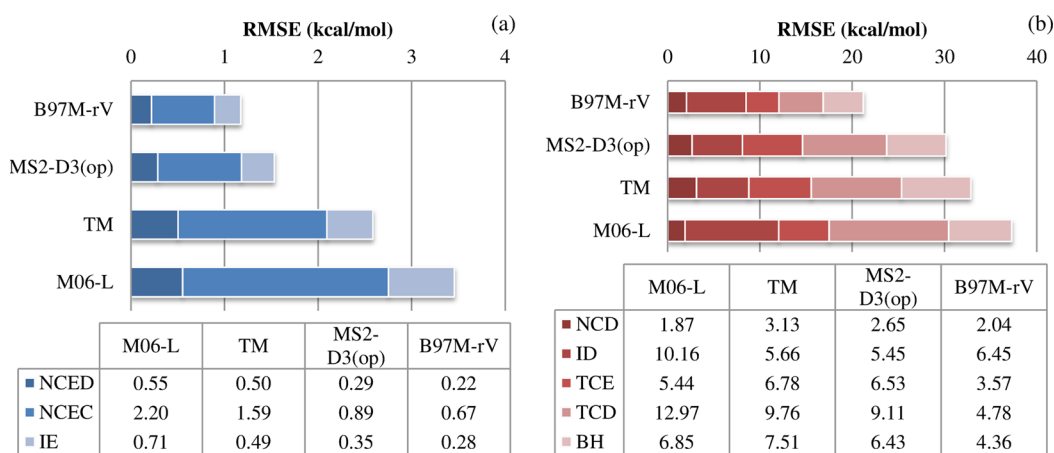


**Figure 4.** Root-mean-square errors (RMSEs) across various datatypes (see Table 3) for the top-performing D3-corrected pure meta-GGA functional examined in this work, as well as three other state-of-the-art pure meta-GGA functionals. For further details, refer to the caption of Figure 3.

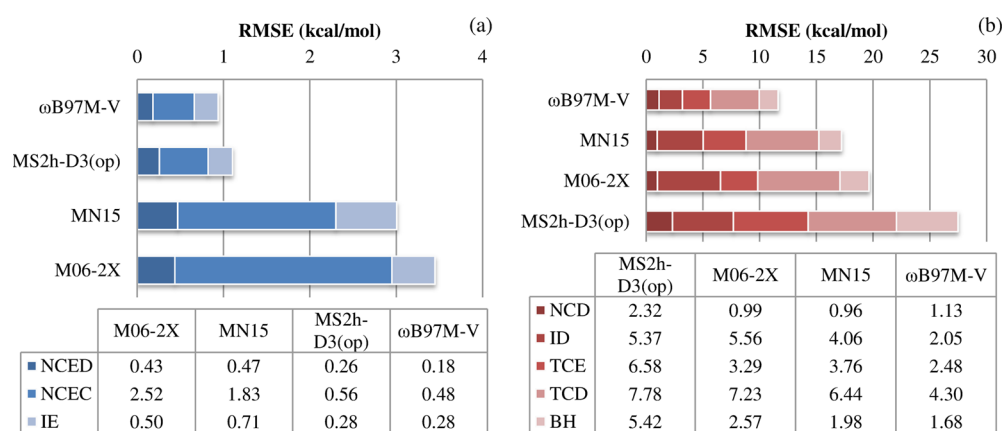


**Figure 5.** Root-mean-square errors (RMSEs) across various datatypes (see Table 3) for the top-performing D3-corrected hybrid meta-GGA functional examined in this work, as well as three other state-of-the-art pure hybrid meta-GGA functionals. For further details, refer to the caption of Figure 3.

reduction in performance for isomerization energies is compensated by a 13% reduction in RMSE across NCEDTest and a 52% reduction in RMSE across NCECTest.

Based on the data in Figure 2, we can make recommendations regarding which fit should be used with each density functional. As a metric of optimality, we use a simple product of the RMSEs across each of the aggregate test sets in Figure 2, i.e. the Product column. It is worth noting that -D2 dramatically underperforms relative to all variants of -D3 for all functionals examined. That being said, even the -D2 corrections represent a major improvement over the base functional. For BLYP, B3LYP, TPSS, and TPSSH, the DFT-D3(op) correction is best, followed by -D3(BJ); for B97, the DFT-D3(op) correction is best, followed by -D3M(BJ); and for revPBE, revPBE0, MS2, and MS2h, DFT-D3(op) is best, followed by -D3(0).

In a similar vein, we can use the data from Figure 2 to make recommendations for the “best” functional/tail combination within each rung of Jacob’s ladder. The top performer among pure GGAs is BLYP-D3(op); at the hybrid GGA level, revPBE0-D3(op); from the pure meta-GGAs, MS2-D3(op); and at the hybrid meta-GGA rung, MS2h-D3(op). Based on the data of Figure 2, these four functional/tail groupings provide the best, most balanced descriptions of noncovalent interactions and isomerization energies, the two datatypes which

empirical dispersion corrections should be capable of improving.

Thus far, we have established two major points: first, when a functional consistently underpredicts intermolecular interactions, the addition of an empirical dispersion correction can greatly improve results; and second, among the dispersion corrections examined, for the systems and density functionals we considered, DFT-D3(op) is best, regardless of the choice of base functional.

To put these results in a broader context, we can compare these “best-in-class” DFT-D3 functionals with state-of-the-art density functionals corresponding to the same rungs of Jacob’s ladder. In Figure 3, the RMSEs across all eight categories of Table 3 are plotted and tabulated for revPBE0-D3(op) and three other hybrid GGAs: ωB97X,<sup>109</sup> ωB97X-D,<sup>22</sup> and ωB97X-V.<sup>110</sup> The left side of Figure 3, (a), contains NCED, NCEC, and IE – the three categories a D3 correction is capable of improving – while the right side, (b), encompasses the remaining datatypes: difficult cases characterized by strong correlation or self-interaction error, as well as thermochemistry and barrier heights. Although revPBE0-D3(op) represents a substantial improvement over ωB97X as far as noncovalent interactions are concerned, the method is somewhat lacking when it comes to the other datatypes: its performance on standard thermochemical problems (TCE) is particularly

lackcluster. That being said, it represents a decent alternative to  $\omega$ B97X-D and even rivals  $\omega$ B97X-V for noncovalent interactions.

The same sort of comparison is made at the pure meta-GGA level in Figure 4. Therein, the top performer from this study, MS2-D3(op), is compared to M06-L,<sup>111</sup> TM,<sup>112</sup> and B97M-rV.<sup>43,113</sup> Here, it seems MS2-D3(op) is actually a viable alternative to standard meta-GGAs; the method generally outperforms both M06-L and TM across the 4399 systems examined. We see a 47% reduction in RMSE across NCED, a 60% reduction in error across NCEC, and a 51% reduction in RMSE across IE for MS2-D3(op) relative to M06-L. This strikes a stark contrast to the performance of the uncorrected MS2 functional, which, relative to M06-L, has a NCED RMSE of 1.27 kcal/mol, a NCEC RMSE of 4.99 kcal/mol, and an IE RMSE of 0.76 kcal/mol; without the DFT-D3(op) correction, MS2 is significantly worse than M06-L across all three categories. This is certainly a testament to the utility of dispersion corrections. That being said, the exemplary performance of MS2-D3(op) – particularly on noncovalent interactions and isomerization energies – is eclipsed by that of B97M-rV, which benefits from the inclusion of nonlocal van der Waals correlation.

As a final example, three popular hybrid meta-GGA functionals – M06-2X,<sup>114</sup> MN15,<sup>115</sup> and  $\omega$ B97M-V<sup>43</sup> – are compared head-to-head with MS2h-D3(op) in Figure 5. Although the DFT-D3(op) dispersion correction allows MS2h to significantly outperform M06-2X and MN15 for standard intermolecular binding energies and isomerization energies – and even come close to the stellar performance of  $\omega$ B97M-V – it can do nothing to rectify the other deficiencies of the method, which manifest themselves in poor performance across the TCE and BH categories in particular. At the hybrid meta-GGA level, the top performer is unambiguously  $\omega$ B97M-V.

## 5. DISCUSSION AND CONCLUSION

In this study, we have introduced a new damping function for the DFT-D3 brand of empirical dispersion corrections. This correction is effectively a generalization of DFT-D3(BJ) wherein the power is treated as an additional parameter and is accordingly named DFT-D3(op), for “optimized-power”-damping. We have parametrized this method for ten distinct density functionals and compared its performance across an external test set to that of existing forms of DFT-D3.

This new approach, -D3(op), consistently yields substantial improvements in the descriptions of molecular clusters, regardless of the base functional with which it is paired. Moreover, it provides a well-balanced description of intermolecular binding energies, equilibrium geometries, and isomerization energies – the three broad classes of data that an empirical dispersion correction can reasonably be expected to improve. Unfortunately, the DFT-D3 correction is not intended to address deficiencies in other aspects – for instance, description of thermochemical properties – of the base functionals to which it is applied. From Figures 3, 4, and 5, it is apparent that there exists at each level of Jacob’s ladder beyond pure GGA at least one functional which will outperform the best comparable DFT-D3 method. This is not particularly surprising; after all, this is not a very fair comparison. Those better methods were built from the ground up; all their components were optimized together, self-

consistently. If anything, it is remarkable just how well this sort of simple post-SCF dispersion correction performs.

The most impressive methods – namely  $\omega$ B97X-V, B97M-rV, and  $\omega$ B97M-V – explicitly include nonlocal correlation, which is a more robust, more powerful treatment of dispersion.<sup>116,117</sup> Similarly, it might be the case that other self-consistent approaches, such as dispersion-corrected potentials<sup>11</sup> and TS-vdW,<sup>118</sup> will outperform the methods introduced here. Such comparisons are beyond the scope of this particular study; the aim here has been simply to introduce an updated, more accurate version of the most computationally economical form of dispersion correction, DFT-D3. In this particular endeavor, we have been successful: for all density functionals examined, DFT-D3(op) yields the best, most balanced performance across the available DFT-D3 dispersion tails.

Specifically, among the pure GGAs examined, BLYP-D3(op) is the standout candidate, offering an unparalleled account of noncovalent interactions. At the hybrid GGA level, revPBE0-D3(op) shines. As far as pure and hybrid meta-GGA functionals go, MS2-D3(op) and MS2h-D3(op) are both quite impressive. For these latter two functionals in particular, the new DFT-D3(op) tail represents a major improvement across all energetic categories over the existing -D3(0) versions. These DFT-D3(op) methods have a significant cost advantage over those incorporating VV10 nonlocal correlation. Moreover, they make relatively small sacrifices on performance across noncovalent interactions and isomerization energies, which makes them well suited for certain applications, e.g. calculations on large or condensed-phase systems, and molecular dynamics.

## ■ ASSOCIATED CONTENT

### Supporting Information

The Supporting Information is available free of charge on the ACS Publications website at DOI: 10.1021/acs.jctc.7b00176.

DFT-D3(op) parametrizations for PBE, PBE0, revTPSS, and revTPSSH and data for rare gas dimers and maximum errors for each method across the various data sets (PDF)

## ■ AUTHOR INFORMATION

### Corresponding Author

\*E-mail: mhg@cchem.berkeley.edu.

### ORCID

Jonathon Witte: 0000-0002-7016-7346

Martin Head-Gordon: 0000-0002-4309-6669

### Author Contributions

J.W. and N.M. contributed equally to this work.

### Notes

The authors declare no competing financial interest.

## ■ ACKNOWLEDGMENTS

This research was supported by the U.S. Department of Energy, Office of Basic Energy Sciences, Division of Chemical Sciences, Geosciences and Biosciences under Award DE-FG02-12ER16362. This work was also supported by the Director, Office of Science, Office of Basic Energy Sciences, of the U.S. Department of Energy under Contract No. DE-AC02-05CH11231 and a subcontract from MURI Grant W911NF-14-1-0359.



## REFERENCES

- (1) Kohn, W.; Sham, L. *Phys. Rev.* **1965**, *140*, A1133–A1138.
- (2) Perdew, J. P.; Schmidt, K. *Jacob's ladder of density functional approximations for the exchange-correlation energy*. AIP Conf. Proc.: Melville, NY, 2001; pp 1–20, DOI: [10.1063/1.1390175](https://doi.org/10.1063/1.1390175).
- (3) Kristyán, S.; Pulay, P. *Chem. Phys. Lett.* **1994**, *229*, 175–180.
- (4) Klimeš, J.; Michaelides, A. *J. Chem. Phys.* **2012**, *137*, 120901.
- (5) Hepburn, J.; Scoles, G.; Penco, R. *Chem. Phys. Lett.* **1975**, *36*, 451–456.
- (6) Ahlrichs, R.; Penco, R.; Scoles, G. *Chem. Phys.* **1977**, *19*, 119–130.
- (7) Wu, Q.; Yang, W. *J. Chem. Phys.* **2002**, *116*, 515.
- (8) Grimme, S. *J. Comput. Chem.* **2004**, *25*, 1463–1473.
- (9) Grimme, S. *J. Comput. Chem.* **2006**, *27*, 1787–1799.
- (10) Grimme, S.; Antony, J.; Ehrlich, S.; Krieg, H. *J. Chem. Phys.* **2010**, *132*, 154104.
- (11) von Lilienfeld, O. A.; Tavernelli, I.; Rothlisberger, U.; Sebastiani, D. *Phys. Rev. Lett.* **2004**, *93*, 153004.
- (12) DiLabio, G. A. *Chem. Phys. Lett.* **2008**, *455*, 348–353.
- (13) Becke, A. D.; Johnson, E. R. *J. Chem. Phys.* **2005**, *122*, 154104.
- (14) Becke, A. D.; Johnson, E. R. *J. Chem. Phys.* **2005**, *123*, 154101.
- (15) Johnson, E. R.; Becke, A. D. *J. Chem. Phys.* **2005**, *123*, 024101.
- (16) Johnson, E. R.; DiLabio, G. A. *Chem. Phys. Lett.* **2006**, *419*, 333–339.
- (17) Tkatchenko, A.; Scheffler, M. *Phys. Rev. Lett.* **2009**, *102*, 073005.
- (18) Dion, M.; Rydberg, H.; Schröder, E.; Langreth, D. C.; Lundqvist, B. I. *Phys. Rev. Lett.* **2004**, *92*, 246401.
- (19) Lee, K.; Murray, D.; Kong, L.; Lundqvist, B. I.; Langreth, D. C. *Phys. Rev. B: Condens. Matter Mater. Phys.* **2010**, *82*, 081101.
- (20) Vydrov, O.; Van Voorhis, T. *Phys. Rev. Lett.* **2009**, *103*, 063004.
- (21) Vydrov, O. A.; Van Voorhis, T. *J. Chem. Phys.* **2010**, *133*, 244103.
- (22) Chai, J.-D.; Head-Gordon, M. *Phys. Chem. Chem. Phys.* **2008**, *10*, 6615–20.
- (23) Grimme, S.; Ehrlich, S.; Goerigk, L. *J. Comput. Chem.* **2011**, *32*, 1456–1465.
- (24) Schröder, H.; Creon, A.; Schwabe, T. *J. Chem. Theory Comput.* **2015**, *11*, 3163–3170.
- (25) Smith, D. G. A.; Burns, L. A.; Patkowski, K.; Sherrill, C. D. *J. Phys. Chem. Lett.* **2016**, *7*, 2197–2203.
- (26) Becke, A. *J. Chem. Phys.* **1997**, *107*, 8554–8560.
- (27) Becke, A. *Phys. Rev. A: At, Mol, Opt. Phys.* **1988**, *38*, 3098–3100.
- (28) Lee, C.; Yang, W.; Parr, R. *Phys. Rev. B: Condens. Matter Mater. Phys.* **1988**, *37*, 785–789.
- (29) Becke, A. D. *J. Chem. Phys.* **1993**, *98*, 5648–5652.
- (30) Stephens, P.; Devlin, F.; Chabalowski, C.; Frisch, M. J. *Phys. Chem.* **1994**, *98*, 11623–11627.
- (31) Perdew, J. P.; Burke, K.; Ernzerhof, M. *Phys. Rev. Lett.* **1996**, *77*, 3865–3868.
- (32) Zhang, Y.; Yang, W. *Phys. Rev. Lett.* **1998**, *80*, 890–890.
- (33) Adamo, C.; Scuseria, G. E.; Barone, V. *J. Chem. Phys.* **1999**, *111*, 2889.
- (34) Tao, J.; Perdew, J.; Staroverov, V.; Scuseria, G. *Phys. Rev. Lett.* **2003**, *91*, 146401.
- (35) Staroverov, V. N.; Scuseria, G. E.; Tao, J.; Perdew, J. P. *J. Chem. Phys.* **2003**, *119*, 12129.
- (36) Sun, J.; Haunschild, R.; Xiao, B.; Bulik, I. W.; Scuseria, G. E.; Perdew, J. P. *J. Chem. Phys.* **2013**, *138*, 044113.
- (37) Gillan, M. J.; Alfè, D.; Michaelides, A. *J. Chem. Phys.* **2016**, *144*, 130901.
- (38) Weigend, F.; Ahlrichs, R. *Phys. Chem. Chem. Phys.* **2005**, *7*, 3297–3305.
- (39) Rappoport, D.; Furche, F. *J. Chem. Phys.* **2010**, *133*, 134105.
- (40) Witte, J.; Neaton, J. B.; Head-Gordon, M. *J. Chem. Phys.* **2016**, *144*, 194306.
- (41) Gill, P. M.; Johnson, B. G.; Pople, J. A. *Chem. Phys. Lett.* **1993**, *209*, 506–512.
- (42) Shao, Y.; Gan, Z.; Epifanovsky, E.; Gilbert, A. T.; Wormit, M.; Kussmann, J.; Lange, A. W.; Behn, A.; Deng, J.; Feng, X.; Ghosh, D.; Goldey, M.; Horn, P. R.; Jacobson, L. D.; Kaliman, I.; Khaliullin, R. Z.; Kuš, T.; Landau, A.; Liu, J.; Proynov, E. I.; Rhee, Y. M.; Richard, R. M.; Rohrdanz, M. A.; Steele, R. P.; Sundstrom, E. J.; Woodcock, H. L.; Zimmerman, P. M.; Zuev, D.; Albrecht, B.; Alguire, E.; Austin, B.; Beran, G. J. O.; Bernard, Y. A.; Berquist, E.; Brandhorst, K.; Bravaya, K. B.; Brown, S. T.; Casanova, D.; Chang, C.-M.; Chen, Y.; Chien, S. H.; Closser, K. D.; Crittenden, D. L.; Diedenhofen, M.; DiStasio, R. A.; Do, H.; Dutoi, A. D.; Edgar, R. G.; Fatehi, S.; Fusti-Molnar, L.; Ghysels, A.; Golubeva-Zadorozhnaya, A.; Gomes, J.; Hanson-Heine, M. W.; Harbach, P. H.; Hauser, A. W.; Hohenstein, E. G.; Holden, Z. C.; Jagau, T.-C.; Ji, H.; Kaduk, B.; Khistyayev, K.; Kim, J.; Kim, J.; King, R. a.; Klunzinger, P.; Kosenkov, D.; Kowalczyk, T.; Krauter, C. M.; Lao, K. U.; Laurent, A. D.; Lawler, K. V.; Levchenko, S. V.; Lin, C. Y.; Liu, F.; Livshits, E.; Lochan, R. C.; Luenser, A.; Manohar, P.; Manzer, S. F.; Mao, S.-P.; Mardirossian, N.; Marenich, A. V.; Maurer, S. A.; Mayhall, N. J.; Neuscamman, E.; Oana, C. M.; Olivares-Amaya, R.; O'Neill, D. P.; Parkhill, J. A.; Perrine, T. M.; Peverati, R.; Prociuk, A.; Rehn, D. R.; Rosta, E.; Russ, N. J.; Sharada, S. M.; Sharma, S.; Small, D. W.; Sodt, A.; Stein, T.; Stück, D.; Su, Y.-C.; Thom, A. J.; Tsuchimochi, T.; Vanovschi, V.; Vogt, L.; Vydrov, O.; Wang, T.; Watson, M. A.; Wenzel, J.; White, A.; Williams, C. F.; Yang, J.; Yeganeh, S.; Yost, S. R.; You, Z.-Q.; Zhang, I. Y.; Zhang, X.; Zhao, Y.; Brooks, B. R.; Chan, G. K.; Chipman, D. M.; Cramer, C. J.; Goddard, W. A.; Gordon, M. S.; Hehre, W. J.; Klamt, A.; Schaefer, H. F.; Schmidt, M. W.; Sherrill, C. D.; Truhlar, D. G.; Warshel, A.; Xu, X.; Aspuru-Guzik, A.; Baer, R.; Bell, A. T.; Besley, N. A.; Chai, J.-D.; Dreuw, A.; Dunietz, B. D.; Furlani, T. R.; Gwaltney, S. R.; Hsu, C.-P.; Jung, Y.; Kong, J.; Lambrecht, D. S.; Liang, W.; Ochsenfeld, C.; Rassolov, V. A.; Slipchenko, L. V.; Subotnik, J. E.; Van Voorhis, T.; Herbert, J. M.; Krylov, A. I.; Gill, P. M.; Head-Gordon, M. *Mol. Phys.* **2015**, *113*, 184–215.
- (43) Mardirossian, N.; Head-Gordon, M. *J. Chem. Phys.* **2016**, *144*, 214110.
- (44) Řezáč, J.; Riley, K. E.; Hobza, P. *J. Chem. Theory Comput.* **2011**, *7*, 2427–2438.
- (45) Řezáč, J.; Riley, K. E.; Hobza, P. *J. Chem. Theory Comput.* **2011**, *7*, 3466–3470.
- (46) Boese, A. D. *J. Chem. Theory Comput.* **2013**, *9*, 4403–4413.
- (47) Boese, A. D. *Mol. Phys.* **2015**, *113*, 1618–1629.
- (48) Boese, A. D. *ChemPhysChem* **2015**, *16*, 978–985.
- (49) Granatier, J.; Pitoňák, M.; Hobza, P. *J. Chem. Theory Comput.* **2012**, *8*, 2282–2292.
- (50) Lao, K. U.; Herbert, J. M. *J. Chem. Phys.* **2013**, *139*, 034107.
- (51) Lao, K. U.; Schäffer, R.; Jansen, G.; Herbert, J. M. *J. Chem. Theory Comput.* **2015**, *11*, 2473–2486.
- (52) Bryantsev, V. S.; Diallo, M. S.; Van Duin, A. C. T.; Goddard, W. A. *J. Chem. Theory Comput.* **2009**, *5*, 1016–1026.
- (53) Goerigk, L.; Grimme, S. *J. Chem. Theory Comput.* **2010**, *6*, 107–126.
- (54) Fanourgakis, G. S.; Aprà, E.; Xantheas, S. S. *J. Chem. Phys.* **2004**, *121*, 2655–2663.
- (55) Anacker, T.; Friedrich, J. *J. Comput. Chem.* **2014**, *35*, 634–643.
- (56) Kozuch, S.; Bachrach, S. M.; Martin, J. M. L. *J. Phys. Chem. A* **2014**, *118*, 293–303.
- (57) Fogueri, U. R.; Kozuch, S.; Karton, A.; Martin, J. M. L. *J. Phys. Chem. A* **2013**, *117*, 2269–2277.
- (58) Yoo, S.; Aprà, E.; Zeng, X. C.; Xantheas, S. S. *J. Phys. Chem. Lett.* **2010**, *1*, 3122–3127.
- (59) Crittenden, D. L. *J. Phys. Chem. A* **2009**, *113*, 1663–1669.
- (60) Marshall, M. S.; Burns, L. A.; Sherrill, C. D. *J. Chem. Phys.* **2011**, *135*, 194102.
- (61) Hohenstein, E. G.; Sherrill, C. D. *J. Phys. Chem. A* **2009**, *113*, 878–886.
- (62) Sherrill, C. D.; Takatani, T.; Hohenstein, E. G. *J. Phys. Chem. A* **2009**, *113*, 10146–10159.
- (63) Takatani, T.; David Sherrill, C. *Phys. Chem. Chem. Phys.* **2007**, *9*, 6106–6114.

- (64) Řezáč, J.; Hobza, P. *J. Chem. Theory Comput.* **2013**, *9*, 2151–2155.
- (65) Mintz, B. J.; Parks, J. M. *J. Phys. Chem. A* **2012**, *116*, 1086–1092.
- (66) Řezáč, J.; Riley, K. E.; Hobza, P. *J. Chem. Theory Comput.* **2012**, *8*, 4285–4292.
- (67) Faver, J. C.; Benson, M. L.; He, X.; Roberts, B. P.; Wang, B.; Marshall, M. S.; Kennedy, M. R.; Sherrill, C. D.; Merz, K. M. *J. Chem. Theory Comput.* **2011**, *7*, 790–797.
- (68) Jurecka, P.; Sponer, J.; Cerný, J.; Hobza, P. *Phys. Chem. Chem. Phys.* **2006**, *8*, 1985–1993.
- (69) Řezáč, J.; Hobza, P. *J. Chem. Theory Comput.* **2012**, *8*, 141–151.
- (70) Witte, J.; Goldey, M.; Neaton, J. B.; Head-Gordon, M. *J. Chem. Theory Comput.* **2015**, *11*, 1481–1492.
- (71) Copeland, K. L.; Tschumper, G. S. *J. Chem. Theory Comput.* **2012**, *8*, 1646–1656.
- (72) Smith, D. G. A.; Jankowski, P.; Slawik, M.; Witek, H. A.; Patkowski, K. *J. Chem. Theory Comput.* **2014**, *10*, 3140–3150.
- (73) Řezáč, J.; Huang, Y.; Hobza, P.; Beran, G. J. O. *J. Chem. Theory Comput.* **2015**, *11*, 3065–3079.
- (74) Li, S.; Smith, D. G. A.; Patkowski, K. *Phys. Chem. Chem. Phys.* **2015**, *17*, 16560–16574.
- (75) Lao, K. U.; Herbert, J. M. *J. Phys. Chem. A* **2015**, *119*, 235–252.
- (76) Temelso, B.; Archer, K. A.; Shields, G. C. *J. Phys. Chem. A* **2011**, *115*, 12034–12046.
- (77) Mardirossian, N.; Lambrecht, D. S.; McCaslin, L.; Xantheas, S. S.; Head-Gordon, M. *J. Chem. Theory Comput.* **2013**, *9*, 1368–1380.
- (78) Karton, A.; O'Reilly, R. J.; Chan, B.; Radom, L. *J. Chem. Theory Comput.* **2012**, *8*, 3128–3136.
- (79) Chan, B.; Gilbert, A. T. B.; Gill, P. M. W.; Radom, L. *J. Chem. Theory Comput.* **2014**, *10*, 3777–3783.
- (80) Tentscher, P. R.; Arey, J. S. *J. Chem. Theory Comput.* **2013**, *9*, 1568–1579.
- (81) Kozuch, S.; Martin, J. M. L. *J. Chem. Theory Comput.* **2013**, *9*, 1918–1931.
- (82) Bauzá, A.; Alkorta, I.; Frontera, A.; Elguero, J. *J. Chem. Theory Comput.* **2013**, *9*, 5201–5210.
- (83) Otero-de-la Roza, A.; Johnson, E. R.; DiLabio, G. A. *J. Chem. Theory Comput.* **2014**, *10*, 5436–5447.
- (84) Steinmann, S. N.; Piemontesi, C.; Delachat, A.; Corminboeuf, C. *J. Chem. Theory Comput.* **2012**, *8*, 1629–1640.
- (85) Karton, A.; Gruzman, D.; Martin, J. M. L. *J. Phys. Chem. A* **2009**, *113*, 8434–8447.
- (86) Gruzman, D.; Karton, A.; Martin, J. M. L. *J. Phys. Chem. A* **2009**, *113*, 11974–11983.
- (87) Wilke, J. J.; Lind, M. C.; Schaefer, H. F.; Császár, A. G.; Allen, W. D. *J. Chem. Theory Comput.* **2009**, *5*, 1511–1523.
- (88) Martin, J. M. L. *J. Phys. Chem. A* **2013**, *117*, 3118–3132.
- (89) Kesharwani, M. K.; Karton, A.; Martin, J. M. L. *J. Chem. Theory Comput.* **2016**, *12*, 444–454.
- (90) Yu, L.-J.; Karton, A. *Chem. Phys.* **2014**, *441*, 166–177.
- (91) Karton, A.; Daon, S.; Martin, J. M. L. *Chem. Phys. Lett.* **2011**, *510*, 165–178.
- (92) Manna, D.; Martin, J. M. L. *J. Phys. Chem. A* **2016**, *120*, 153–160.
- (93) Curtiss, L. A.; Raghavachari, K. *J. Chem. Phys.* **1991**, *94*, 7221–7230.
- (94) Zhao, Y.; González-García, N.; Truhlar, D. G. *J. Phys. Chem. A* **2005**, *109*, 2012–2018.
- (95) Zhao, Y.; Lynch, B. J.; Truhlar, D. G. *Phys. Chem. Chem. Phys.* **2005**, *7*, 43–52.
- (96) Lynch, B. J.; Zhao, Y.; Truhlar, D. G. *J. Phys. Chem. A* **2003**, *107*, 1384–1388.
- (97) Grimme, S.; Kruse, H.; Goerigk, L.; Erker, G. *Angew. Chem., Int. Ed.* **2010**, *49*, 1402–1405.
- (98) Goerigk, L.; Grimme, S. *J. Chem. Theory Comput.* **2011**, *7*, 291–309.
- (99) Krieg, H.; Grimme, S. *Mol. Phys.* **2010**, *108*, 2655–2666.
- (100) O'Reilly, R. J.; Karton, A. *Int. J. Quantum Chem.* **2016**, *116*, 52–60.
- (101) Karton, A.; Martin, J. M. L. *Mol. Phys.* **2012**, *110*, 2477–2491.
- (102) Karton, A.; Schreiner, P. R.; Martin, J. M. L. *J. Comput. Chem.* **2016**, *37*, 49–58.
- (103) Karton, A.; Goerigk, L. *J. Comput. Chem.* **2015**, *36*, 622–632.
- (104) Yu, L.-J.; Sarrami, F.; O'Reilly, R. J.; Karton, A. *Chem. Phys.* **2015**, *458*, 1–8.
- (105) Zheng, J.; Zhao, Y.; Truhlar, D. G. *J. Chem. Theory Comput.* **2007**, *3*, 569–582.
- (106) Karton, A.; Tarnopolsky, A.; Lamère, J. F.; Schatz, G. C.; Martin, J. M. L. *J. Phys. Chem. A* **2008**, *112*, 12868–12886.
- (107) Yu, L.-J.; Sarrami, F.; O'Reilly, R. J.; Karton, A. *Mol. Phys.* **2016**, *114*, 21–33.
- (108) Schröder, H.; Hühnert, J.; Schwabe, T. *J. Chem. Phys.* **2017**, *146*, 044115.
- (109) Chai, J.-D.; Head-Gordon, M. *J. Chem. Phys.* **2008**, *128*, 084106.
- (110) Mardirossian, N.; Head-Gordon, M. *Phys. Chem. Chem. Phys.* **2014**, *16*, 9904–9924.
- (111) Zhao, Y.; Truhlar, D. G. *J. Chem. Phys.* **2006**, *125*, 194101.
- (112) Tao, J.; Mo, Y. *Phys. Rev. Lett.* **2016**, *117*, 73001.
- (113) Mardirossian, N.; Head-Gordon, M. *J. Chem. Phys.* **2015**, *142*, 074111.
- (114) Zhao, Y.; Truhlar, D. G. *Theor. Chem. Acc.* **2008**, *120*, 215–241.
- (115) Yu, H. S.; He, X.; Li, S. L.; Truhlar, D. G. *Chem. Sci.* **2016**, *7*, 5032–5051.
- (116) Goerigk, L. *J. Chem. Theory Comput.* **2014**, *10*, 968–980.
- (117) Hujo, W.; Grimme, S. *J. Chem. Theory Comput.* **2011**, *7*, 3866–3871.
- (118) Tkatchenko, A.; DiStasio, R. A.; Car, R.; Scheffler, M. *Phys. Rev. Lett.* **2012**, *108*, 236402.